frontiers in Cellular Neuroscience

ORIGINAL RESEARCH
published: 12 June 2019
doi: 10.3389/fncel.2019.00267

Acetylcholine Release Inhibits Distinct Excitatory Inputs Onto Hippocampal CA1 Pyramidal Neurons via Different Cellular and Network Mechanisms

*Priyodarshan Goswamee and A. Rory McQuiston**

Department of Anatomy and Neurobiology, School of Medicine, Virginia Commonwealth University, Richmond, VA, United States

In hippocampal CA1, muscarinic acetylcholine (ACh) receptor (mAChR) activation via exogenous application of cholinergic agonists has been shown to presynaptically inhibit Schaffer collateral (SC) glutamatergic inputs in stratum radiatum (SR), and temporoammonic (TA) and thalamic nucleus reuniens (RE) glutamatergic inputs in stratum lacunosum-moleculare (SLM). However, steady-state uniform mAChR activation may not mimic the effect of ACh release in an intact hippocampal network. To more accurately examine the effect of ACh release on glutamatergic synaptic efficacy, we measured electrically evoked synaptic responses in CA1 pyramidal cells (PCs) following the optogenetic release of ACh in genetically modified mouse brain slices. The ratio of synaptic amplitudes in response to paired-pulse SR stimulation (stimulus 2/stimulus 1) was significantly reduced by the optogenetic release of ACh, consistent with a postsynaptic decrease in synaptic efficacy. The effect of ACh release was blocked by the M_3 receptor antagonist 4-DAMP, the $GABA_B$ receptor antagonist CGP 52432, inclusion of GDP-β-S, cesium, QX314 in the intracellular patch clamp solution, or extracellular barium. These observations suggest that ACh release decreased SC synaptic transmission through an M_3 muscarinic receptor-mediated increase in inhibitory interneuron excitability, which activate $GABA_B$ receptors and inwardly rectifying potassium channels on CA1 pyramidal cells. In contrast, the ratio of synaptic amplitudes in response to paired-pulse stimulation in the SLM was increased by ACh release, consistent with presynaptic inhibition. ACh-mediated effects in SLM were blocked by the M_2 receptor antagonist AF-DX 116, presumably located on presynaptic terminals. Therefore, our data indicate that ACh release differentially modulates excitatory inputs in SR and SLM of CA1 through different cellular and network mechanisms.

Keywords: acetylcholine release, excitatory input modulation, CA1, interneurons, $GABA_B$, GIRK channels

OPEN ACCESS

Edited by:
Dirk Feldmeyer, Julich Research Centre, Germany

Reviewed by:
Takashi Tominaga, Tokushima Bunri University, Japan
Lang Wang, Zhejiang University, China

****Correspondence:***
A. Rory McQuiston
amcquiston@vcu.edu

Specialty section:
This article was submitted to Cellular Neurophysiology, a section of the journal Frontiers in Cellular Neuroscience

Received: *12 March 2019*
Accepted: *29 May 2019*
Published: *12 June 2019*

Citation:
Goswamee P and McQuiston AR (2019) Acetylcholine Release Inhibits Distinct Excitatory Inputs Onto Hippocampal CA1 Pyramidal Neurons via Different Cellular and Network Mechanisms. Front. Cell. Neurosci. 13:267. doi: 10.3389/fncel.2019.00267

INTRODUCTION

Medial septum and diagonal band of Broca complex (MS/DBB) cholinergic neurons project to the hippocampus where they influence attention, learning, and memory (Hasselmo, 2006), and synaptic plasticity (Zhenglin and Yakel, 2011). In Alzheimer's disease, MS/DBB cholinergic neurons are among the first cells to degenerate (Hampel et al., 2018), which underscores their significance

in the pathophysiology of the disease and highlights a need for a better understanding of the mechanisms by which MS/DBB cholinergic inputs affect hippocampal function.

Medial septum and diagonal band of Broca complex cholinergic inputs affect hippocampal function through a variety of cellular and network mechanisms. In hippocampal CA1, activation of muscarinic and nicotinic receptors affect the excitability of pyramidal cells (PCs) (Cole and Nicoll, 1983), inhibitory interneurons (Frazier et al., n.d.; Pitler and Alger, 1992; Jones and Yakel, 1997; McQuiston and Madison, 1999a,b,c) and astrocytes (Araque et al., 2002). At the synapse, presynaptic nicotinic receptor activation has been shown to facilitate the release of glutamate onto CA1 PCs (Ji et al., 2001; Maggi et al., 2003; Sola et al., 2006) whereas activation of presynaptic muscarinic receptor has been shown to inhibit glutamate release (Valentino and Dingledine, 1981; Hasselmo and Schnell, 1994; Qian and Saggau, 1997).

Hippocampal CA1 PCs are primarily driven by three excitatory glutamatergic inputs. Two of these excitatory inputs are located in the stratum lacunosum-moleculare (SLM) and synapse on distal apical CA1 PC dendrites – the temporoammonic pathway (TA) from the entorhinal cortex and inputs from the thalamic nucleus reuniens (RE). The other excitatory input, the Schaffer-collaterals (SC), originate in hippocampal CA3 and synapse on the proximal apical and basal dendrites of CA1 PCs in the stratum radiatum (SR) and stratum oriens (SO), respectively. A proportionately larger presynaptic muscarinic receptor-mediated inhibition has been observed in the SC pathway of SR compared to inhibition of inputs located in the SLM (Hasselmo and Schnell, 1994). However, these studies were conducted using exogenous uniform activation of muscarinic receptors in rat brain slices. This experimental paradigm may not accurately measure the influence of cholinergic inputs on hippocampal CA1 synaptic function as MS/DBB cholinergic inputs and acetylcholinesterase are not uniformly distributed in the hippocampus (Aznavour et al., 2002; Franklin and Paxinos, n.d.). Physiological measures of acetylcholine levels in the hippocampus match the anatomical data as acetylcholine concentrations appear to be larger in the stratum pyramidale compared to all other layers in hippocampal CA1 during theta rhythm (Zhang et al., 2010). Thus, muscarinic receptors located on different subsets of presynaptic glutamatergic terminals may be exposed to different concentrations of acetylcholine following release from MS/DBB terminals. This would impact the magnitude of cholinergic presynaptic inhibition following the release of ACh from synaptic terminals.

Therefore, we assessed the impact of ACh release on glutamatergic synaptic transmission in SR and SLM of hippocampal CA1. To do this we optogenetically released ACh from MS/DBB cholinergic terminals expressing the red-shifted optogenetic excitatory protein ReaChR and measured the effect of ACh release on paired electrically evoked glutamatergic postsynaptic excitatory responses in hippocampal CA1 PCs. Here, we report that optogenetic activation of ACh release indirectly reduced paired-pulse ratio (PPR, stimulus 2/stimulus 1) in SR by an M_3-muscarinic receptor-mediated increase in excitability of inhibitory interneurons. The combined increase in interneuron excitability coupled with SR excitatory input resulted in the activation of postsynaptic $GABA_B$-receptors and inwardly rectifying potassium channels in the CA1 PCs. In contrast, ACh release appeared to result in presynaptic inhibition of terminals in SLM via an M_2-dependent mechanism. Therefore, our data suggest that ACh release has different cellular and network mechanisms of action on glutamatergic neurotransmission in the SR and SLM of hippocampal CA1.

MATERIALS AND METHODS

Pharmacological Agents

All chemicals were purchased from ThermoFisher scientific unless otherwise indicated. VU 0255035 (highly selective muscarinic M_1 receptor antagonist), 4-DAMP (Muscarinic M3 receptor antagonist), PD 102807 (selective M4 receptor antagonist), AF-DX 116 (selective M2-muscarinic receptor antagonist), Baclofen ($GABA_B$ receptor antagonist), QX 314 chloride (intracellular sodium channel blocker), and CGP 52432 (selective $GABA_B$ receptor antagonist) were obtained from Tocris Bioscience (Ellisville, MO, United States). GDP-β-S was purchased from Sigma. Bicuculline methochloride (competitive $GABA_A$ receptor antagonist) was purchased from helloBio (Montogomery, NJ, United States). Biocytin (B-1592) was purchased from Life Technologies (Invitrogen).

Animals

The B6.Cg-Gt(ROSA)26Sortm2.2Ksvo/J (ReaChR JAX Stock No. 026294) and 134 B6; 129S6-Chattm1(cre)Lowl/J (Chat-cre, JAX Stock No. 006410) mice used in these studies were housed in an animal care facility approved by the American Association for the Accreditation of Laboratory Animal Care (AAALAC). Animal experimental procedures followed a protocol approved by the Institutional Animal Care and Use Committee of Virginia Commonwealth University (AD 20205). This protocol adhered to the ethical guidelines described in The Care and Use of Laboratory Animals, 8th Edition. Efforts were made to minimize animal suffering and to reduce the number of animals used.

Breeding Strategy

Homozygous chat-cre mice were crossed with homozygous ReaChR mice. The resulting offspring were heterozygous for both alleles. In some experiments, these progeny mice, which were heterozygous for both alleles, were further crossed to achieve homozygosity in both alleles. Animals that expressed at least one copy of the mutant alleles in both loci were utilized for physiological experiments and were identified by genotyping using specific primers for the mutant alleles (**Table 1**).

In brain slices prepared from some animals, ectopic expression of mCitrine was observed in what appeared to be astrocytes. Data from such animals were not included in analysis.

Preparation of Brain Slices

Adult mice (30–180 days old) were deeply anesthetized with an intraperitoneal injection of ketamine (200 mg/kg) and xylazine

TABLE 1 | PCR primers used to genotype mouse crosses.

Mouse strain	Forward primer	Reverse primer	Source
ReaChR 026294	5′CCAACAGCAAAGGAAAGAGC 3′	5′TTCAAGAAGCTTCCAGAGGAAC 3′	Custom
Chat-Cre 006410	5′ CCAACAGCAAAGGAAAGAGC 3′	5′ TTCAAGAAGCTTCCAGAGGAAC 3′	Custom

(20 mg/kg), following which, the animals were transcardially perfused with ice-cold sucrose saline [consisting of (in mM): Sucrose 230, KCl 3.0, $CaCl_2$ 1.2, $MgCl_2$ 6, Na_2HPO_4 1.2, $NaHCO_3$ 25, glucose 25]. The brain was removed and sectioned to prepare coronal MS/DBB or horizontal brain slices that contained mid-temporal hippocampus. Slices were cut at 350 μm on a Leica VT1200 (Leica Microsystems, Buffalo Grove, IL, United States) and incubated in a holding chamber containing artificial cerebrospinal fluid (aCSF) [(in mM): NaCl 125, KCl 3.0, $CaCl_2$ 1.2, $MgCl_2$ 1.2, $NaHPO_4$ 1.2, $NaHCO_3$ 25, glucose 25 bubbled with 95% O_2/5% CO_2] at 32°C for at least 30 min before commencement of electrophysiological experiments.

Light-Evoked Release of Acetylcholine From MS/DBB Cholinergic Axon Terminals

Cholinergic terminals expressing ReaChR-mCitrine were stimulated by 40 yellow light pulses delivered at 4–5 Hz (10 ms in duration). The light pulses were generated from a UHP-T-LED-White light-emitting diode (LED) (Prizmatix Modiin-Ilite, Givat Shmuel, Israel). The white light exiting the LED was filtered by an HQ575/50x excitation filter (Chroma technology) and was focused into the epi-illumination light path of the Olympus BX51WI microscope and back aperture of a 10× water immersion objective (0.3 NA) using an optiblock beam combiner (Prizmatix) and a dichroic mirror (700dcxxr, Chroma Technology) in the filter turret.

Immunofluorescent and Functional Verification of ReaChR Expression in Septal Cholinergic Neurons

To assess the effect of light exposure on the membrane potential of cholinergic neurons, we performed electrophysiological recordings from mCitrine-expressing MS/DBB cholinergic neurons in acute coronal tissue slices taken from the brains of ChReaChR mice. Biocytin was included in the intracellular patch solution for *post hoc* identification of the neurons from which we recorded. Following electrophysiological recordings, brain slices were drop-fixed in 4% paraformaldehyde for at least 24 h. Subsequently, slices were washed and incubated in a blocking/permeabilizing buffer (1X PBS supplemented with 0.2% bovine serum albumin and Triton-X 100) for 24 h. Sections were then incubated for 3 days at 4°C with 1:200 dilution of a Goat polyclonal anti-ChAt antibody (EMD Millipore, Cat# AB144P). Slices were then washed three times with phosphate-buffered saline and incubated with 1:200 dilution of Donkey anti-Goat 568 (Thermo Fisher, Cat # A-11057) and 1:1000 dilution of streptavidin Alexa Fluor 633 (Thermo Fisher, Cat # S-11226). Processed slices were then imaged using a Zeiss LSM710 confocal microscope (Carl Zeiss, Jena, Germany).

Because mCitrine fluorescent intensity was poor and could not be reliably amplified using an anti-GFP antibody in 350 μm thick brain slice, we performed a separate set of experiments, independent of the physiological studies, to determine the degree of ChAT and mCitrine colocalization. To do this, ChReaChR mice ($n = 2$) were deeply anesthetized with ketamine (200 mg/kg) and xylazine (20 mg/kg) and then trans-cardially perfused with 4% paraformaldehyde. Brains were removed and incubated in 4% paraformaldehyde for 24 h. After 24 h, the brains were placed in 30% sucrose solution for 48 h. Subsequently, 50 μm thick coronal sections of the MS/DBB were prepared using a cryostat (Thermo Scientific, MA, United States). These sections were processed for immunofluorescence utilizing Goat polyclonal anti-ChAt antibody and a 1:500 dilution of GFP-Tag polyclonal antibody conjugated with AlexaFluor 488. Stained sections were imaged using a Zeiss LSM710 confocal microscope (Carl Zeiss, Jena, Germany) to determine overlap between ChAT positive and mCitrine positive soma.

Electrophysiology

Whole cell patch clamp recordings were conducted on medial septum/diagonal band of Broca (MS/DBB) cholinergic neurons, hippocampal CA1 interneurons, and PCs. For these experiments, patch pipettes (3–4 MΩ) pulled from borosilicate glass (8250 1.65/1.0 mm) on a Sutter P-1000 pipette puller and were filled with intracellular recording solution that contained either a potassium-based recording solution [(in mM): $KMeSO_4$ 145, NaCl 8, Mg-ATP 2, Na-GTP 0.1, HEPES 10, EGTA 0.1] or a Cesium-based recording solution [(in mM): $CsMeSO_4$ 120, NaCl 8, Mg-ATP 2, Na-GTP 0.1, HEPES 10, Cs-BAPTA 10, QX-314 Chloride 10]. In some experiments with the potassium recording solution, the GTP was replaced with 5 μM GDP-β-S, an inhibitor of G-protein coupled receptor. 0.1% biocytin was included in the intracellular recording solution in a subset of experiments for *post hoc* identification of the recorded cell. Membrane potentials or excitatory postsynaptic currents (EPSCs) were measured with a Model 2400 patch clamp amplifier (A-M Systems, Port Angeles, WA, United States) and converted into a digital signal by a PCI-6040E A/D board (National Instruments, Austin, TX, United States). WCP Strathclyde Software (courtesy of Dr. J. Dempster, Strathclyde University, Glasgow, Scotland) was used to collect and store membrane potential or EPSC responses on a PC computer. For all voltage clamp experiments, series resistance was compensated to approximately 70%, and experiments in which the access resistance changed by more than approximately 20% were discarded. To evoke paired-pulse responses in hippocampal CA1 principal cells, bipolar platinum–iridium stimulating electrodes (approx. 100 kΩ, FHC Inc.,

Bowdoin, ME, United States) were placed in SC (in stratum radiatum) or TA/RE pathway (SLM). A pair of electrical pulses (40–120 μs pulse width, 50–100 μAmp), 50 ms in interval, were used to stimulate the axons. Stimulation currents were titrated to achieve responses that were approximately 70% of the maximum EPSC amplitudes. The time interval between successive paired-pulse stimulation was 45 s. The PPR was calculated by dividing the averaged peak EPSC amplitude in response to the second pulse (P2) by that of the first pulse (P1) (P2/P1). Light-evoked ACh release was achieved by delivering a 5 Hz train of 40 yellow light pulses (10 ms each) immediately before the electrical paired-pulse. This stimulation paradigm will be referred to as "Light ON" for the remainder of the manuscript. In the same cells, PPR was calculated in the absence of light stimulation. These responses will be termed as "Light OFF". Data presented shows averaged responses from five consecutive Light OFF and Light ON stimulations. Because optogenetic release of ACh in slices is prone to rapid hydrolyzation due to acetylcholinesterase activity, we conducted some experiments in presence of 0.1 μM Donepezil, an acetylcholinesterase inhibitor, as utilized by others (Alger et al., 2014).

Experimental Design and Statistical Analysis

Data analysis was performed with OriginPro 2018 (OriginLab Corp., Northampton, MA, United States) and Excel (Microsoft, Redmond, WA). Statistics were performed using GraphPad Prizm software (La Jolla, CA, United States). A total of 39 mice (21 males and 18 females) were utilized in the study. At least three animals were utilized for every experiment. Numbers of paired recording performed for every experiment was aimed to attain 80% power, determined using GraphPad StatMate 2.0 (San Diego, CA, United States). The clustering of cells per mouse was random, and no data point was utilized in more than one analysis. The precise number of cells per animal sampled is indicated in the results. Comparison of PPR amplitudes were conducted within cell and had only one variable (i.e., light-evoked release of ACh) and therefore, the statistical significances of the results were determined using paired two-tailed *t*-tests. Statistical differences of results between two groups of data collected from separate groups of cells [**Figures 5D** (lower panel), 6A] were compared using two-tailed unpaired *t*-tests. Differences were determined to be statistically significant for *p*-values less than 0.05. All data are reported as the mean, standard error of the mean (SEM). Asterisks were used as follows unless otherwise noted, $^{***}p < 0.001$, $^{**}p < 0.01$, $^{*}p < 0.05$.

RESULTS

Immunofluorescent and Functional Verification of ReaChR Expression in the MS/DBB Cholinergic Pathway

To optogenetically release ACh from MS/DBB cholinergic terminals in mouse hippocampal brain slices, we crossed a driver mouse line that expressed Cre-recombinase under the control of the choline acetyltransferase gene (ChAt-Cre) (Rossi et al., 2011) to a reporter mouse line that contained a Cre-dependent coding sequence for a red-shifted designer channelrhodopsin (ReaChR-mCitrine) knocked into the Rosa26 locus (Rosa-CAG-LSL-ReaChR-mCitrine-WPRE) (Lin et al., 2013; Hooks et al., 2015). The selective expression of ReaChR in MS/DBB cholinergic neurons was confirmed by measuring light-evoked depolarizations in mCitrine fluorescent neurons of MS/DBB brain slices using whole cell patch clamp techniques (**Figure 1A**, upper panel). With resting membrane potential near −60 mV, 600 ms duration light-evoked responses were often accompanied by 1–2 action potentials (APs) that occurred near the beginning of the light pulse. We further assessed the electrophysiological responses to hyperpolarizing and depolarizing current steps (**Figure 1A**, lower panel). Membrane potential hyperpolarizing responses displayed a delayed return to baseline membrane potentials (200–300 ms, arrowhead) after termination of the current pulse. Furthermore, MS/DBB cholinergic cells exhibited strong spike frequency adaptation in response to positive current injection steps. These observations were consistent with previous descriptions of cholinergic neurons in the MS/DBB (Brazhnik and Fox, 1997; Wu, 2004; Wu et al., 2004).

By including 0.2% biocytin in the intracellular patch pipette solution, we were able to *post hoc* identify the cell from which we recorded. To confirm whether the recorded cell was cholinergic, brain slices were fixed and processed for immunofluorescence using an antibody against choline acetyltransferase (ChAT). Analysis of the tissue revealed that the recorded neuron in the in MS region was also positive for ChAT (**Figure 1B**).

In a separate set of experiments, we determined the proportion of ChAT positive neurons (identified using the anti-ChAT antibody) that colocalized with expression of mCitrine in the MS/DBB brain slices. In these experiments, the endogenous mCitrine fluorescent signal was amplified using an anti-GFP antibody conjugated to AlexaFluor 488. As shown in **Figure 1C**, all the neurons that expressed ChAT were also expressing mCitrine, and vice-versa.

Functional Verification of Light-Evoked ACh Release in Hippocampus Slices

We next confirmed that light stimuli released ACh in hippocampal slices. Light stimuli (4 or 5 Hz train of yellow light pulses) produced the expected depolarizing (**Figure 2A**), hyperpolarizing (**Figure 2C**) or biphasic responses (**Figure 2D**) in CA1 interneurons located in the stratum oriens and radiatum as has been previously reported by our laboratory when using higher stimulation frequencies and the optogenetic protein oChIEF (Bell et al., 2013, 2015a,b). We morphologically confirmed the interneuron identity of a subset of neurons from which we recorded by including biocytin in the patch pipette (**Figure 2B**). Furthermore, the cholinesterase inhibitor donepezil (0.1 μM) increased response amplitudes in the recorded neuron (**Figure 2D**), whereas the muscarinic receptor antagonist atropine (5 μM) inhibited the responses (**Figures 2A,C,D**). Some cells (**Figure 2D**) responded with complex waveforms in which faster atropine-resistant responses were superimposed on the

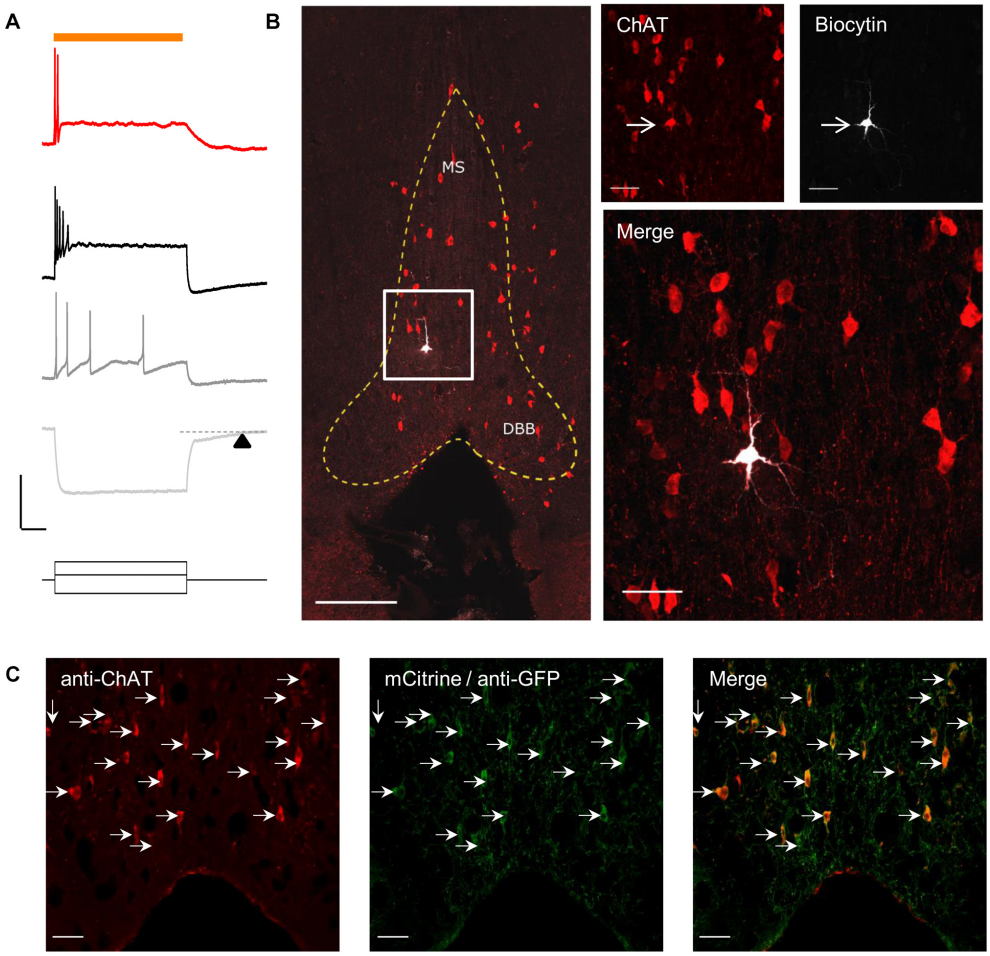

FIGURE 1 | Red-shifted optogenetic protein (ReachR) was functionally expressed in MS/DBB cholinergic neurons and terminals of Chat-cre × ReaChR-mCitrine mice. **(A)** Upper, Representative trace (red) showing a MS/DBB cholinergic neuron that depolarized and fired action potentials (APs) in response to a 600 ms long pulse of yellow light (indicated by orange bar); Lower, The membrane potential changes in the same cell in response to injection of –200 pA (light gray), +75 pA (dark gray), and +275 pA (black) current steps. The time delay in returning to baseline (dashed line) following hyperpolarization in response to a negative current injection is indicated by the black triangle; Scale bars: x = 200 ms and y = 20 mV. **(B)** Left, Image of the MS/DBB in a coronal brain slice: anti-choline acetyl transferase (ChAT, red); biocytin filled cell (white) from **(A)**; scale bar = 100 μm. The MS/DBB area is marked by yellow dashed lines. Right, magnified z-projection image of the same region (indicated by white box in left) showing the biocytin filled cell was positive for ChAT (red); scale bar = 50 μm. **(C)** Immunofluorescence performed on 50 μm coronal sections of the MS/DBB showed that ChAT positive neurons (red), indicated by white arrows, were also positive for mCitrine expression (green), and vice-versa; Scale bar = 50 μm.

atropine-sensitive slower waveform. Although not directly tested, the kinetic properties of the atropine resistant responses were consistent with nicotinic responses observed previously (Bell et al., 2011). Based on these observations, we concluded that the animal cross was suitable for studying the effects of ACh release in hippocampal slices.

Optogenetic Release of ACh Had Differing Effects on PPR on Input in the SR and SLM

Previous studies have reported that activation of presynaptic muscarinic receptors causes inhibition of the SC and TA inputs (Hasselmo and Schnell, 1994; Fernández de Sevilla and Buño, 2003; Thorn et al., 2017). Alternatively, activation of nicotinic receptors has been shown to enhance glutamate release and reduce PPR in the SC (Maggi et al., 2003). However, immediate effects of the release of ACh on presynaptic cholinergic receptors has only been investigated for muscarinic receptors on SC inputs (Buño et al., 2006). Therefore, using physiologically relevant optogenetic stimulation rates of MS/DBB cholinergic axon terminals (>4 Hz) (Simon, 2006; Zhang et al., 2011), in hippocampal CA1, we investigated the effect of ACh release on glutamatergic neurotransmission in the SR and SLM. To do this we measured the amplitudes and PPRs of EPSCs in CA1 PCs following stimulation of SR and SLM inputs. We compared EPSC amplitudes and PPRs measured under control stimulation (light OFF) with those following the optogenetic stimulation of the

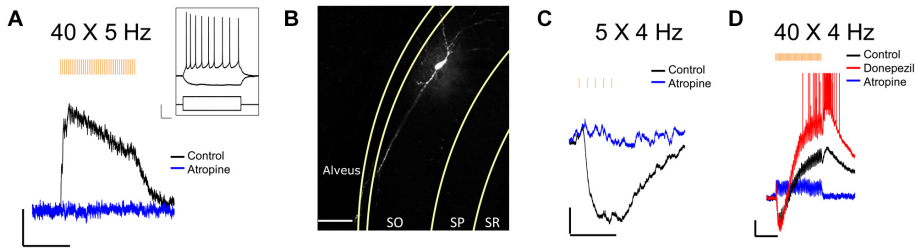

FIGURE 2 | Optogenetically released ACh in hippocampal slice evokes predictable response types in CA1 interneurons. **(A)** Representative trace showing a stratum oriens interneuron depolarized in response to 40 X 5 Hz stimulation; Scale bar: x = 5000 ms, y = 2 mV; Inset changes in membrane potential of the same neuron in response to depolarizing (+200 pA) and hyperpolarizing (–200 pA) current injections; Scale bar: x = 100 ms, y = 20 mV. **(B)** Fluorescent image of the same neuron as in **(A)** after *post hoc* staining with streptavidin conjugated to AlexaFluor 633 to label biocytin; Scale bar = 50 microns. **(C,D)** Representative traces showing ACh-mediated hyperpolarization (**C**; scale bar: x = 1000 ms; y = 2 mV), and biphasic response (**D**; scale bars: x = 5000 ms; y = 2 mV).

cholinergic terminals (light ON). In the "Light ON" condition, a 5 Hz train of 40 pulses of yellow light (10 ms pulse width) was delivered immediately before stimulating SR or SLM inputs with a pair of electrical stimuli (40–120 μs in duration and 50 ms interval). **Figures 3A,B** schematically illustrate our experimental paradigm. Optogenetic release of ACh prior to paired-pulse electrical stimulation of SR inputs reduced the amplitude of the second EPSC [**Figures 3C,E** (right) Light OFF: −138.8 ± 11.95 vs. Light ON: −108 ± 9.301; $p < 0.0001$], but had no significant effect on the first EPSC amplitude (**Figures 3C,E** (left) Light OFF: −89.95 ± 9.104 vs. Light ON: −86.47 ± 7.908; $p = 0.3725$). This resulted in a significant reduction of the paired-pulse ratio in SR following ACh release (**Figure 3D**; $p < 0.001$; $t = 9.041$; df = 20; $n = 21$ cells from nine animals).

In contrast, optogenetic release of ACh prior to electrical stimulation of SLM inputs significantly reduced the amplitudes of both the first (Light OFF: −57.34 ± 9.002 vs. Light ON: −38.93 ± 6.073; $p = 0.0007$) and the second EPSCs (Light OFF: −66.92 ± 9.239 vs. Light ON: −56.53 ± 7.977; $p = 0.0062$) (**Figures 3F,H**). Furthermore, ACh release caused an increase in the PPR of inputs in the SLM (**Figures 3F,G**; $p = 0.0096$; $t = 3.194$; df = 10; $n = 11$ cells from six animals).

Although most experiments were conducted in the presence of the acetylcholinesterase inhibitor donepezil (100 μM), a significant reduction in PPR in SR was also observed in donepezil's absence (Light OFF: 1.662 ± 0.047 vs. Light ON: 1.411 ± 0.045; $p = 0.0029$; $t = 4.829$; df = 6; $n = 7$ from four animals). However, we failed to see an effect of ACh release on PPR in SLM in the absence of donepezil (Light OFF: 1.278 ± 0.038 vs. Light ON: 1.346 ± 0.058; $p = 0.0618$; $t = 2.221$; df = 7; $n = 8$ from four animals). Therefore, these results indicated that synaptically released ACh had distinct effects on glutamatergic neurotransmission in the SR and SLM.

Muscarinic ACh Receptor Activation Mediates the Effect of ACh Release on Neurotransmission in the SR and SLM

We next investigated the type of cholinergic receptors that underlie the effect of ACh release on synaptic transmission in SR and SLM inputs. In the SR, the muscarinic receptor antagonist atropine (5 μM) blocked the ACh mediated reduction of PPR (**Figure 4A**, $p = 0.7629$; $t = 0.3137$; df = 7; $n = 8$ cells from three animals). In contrast, inclusion of the α7 nicotinic receptor antagonist MLA (0.1 μM) in the extracellular solution had no effect (**Figure 4B**; $p = 0.0007$; $t = 7.418$; df = 5; $n = 6$ cells from three animals). Similarly, in the SLM atropine blocked the ACh-mediated increase in PPR (**Figure 4C**, $p = 0.7159$; $t = 0.3791$; df = 7; $n = 8$ cells from three animals), whereas MLA had no effect (**Figure 4D**; $p = 0.0036$; $t = 8.368$; df = 3; $n = 4$ cells from three animals). Therefore, release of ACh inhibited glutamatergic inputs in the SR and SLM via the activation of muscarinic cholinergic receptors.

Activation of Postsynaptic $GABA_B$ Receptors Mediate the Effect of ACh Release on SC Neurotransmission

One possible mechanism to explain the ACh-mediated effect on PPR in the SR is through an indirect increase in the excitability of CA1 GABAergic interneurons (Pitler and Alger, 1992; Parra et al., 1998; McQuiston and Madison, 1999a). To test this possibility, we inhibited $GABA_A$ and $GABA_B$ receptors through bath application of 25 μM bicuculline (BIC) and 2 μM CGP 52432, respectively. As shown in **Figure 5A**, bath application with BIC and CGP 52432 blocked the ACh-mediated reduction of PPR ($p = 0.2440$; $t = 1.292$; df = 6; $n = 7$ cells from four animals). To determine the relative contribution of these two GABA receptor subtypes, we repeated the experiments with either BIC or CGP 52432 alone. Bath application of CGP 52432 alone was sufficient to block the ACh mediated reduction of PPR (**Figure 5C**; $p = 0.8332$; $t = 0.2186$; df = 7; $n = 8$ cells from four animals). In contrast, ACh release in the presence of BIC resulted in a reduction in PPR (**Figure 5B**; $p = 0.0023$; $t = 5.054$; df = 6; $n = 7$ cells from three animals). Therefore, these data suggest that the optogenetic release of ACh increased the excitability of interneurons and suppressed the pathway in SR by the activation of $GABA_B$ receptors. $GABA_B$ receptors are expressed on both presynaptic SC terminals and postsynaptic CA1 PCs. Thus, GABA release could inhibit synaptic transmission in SR through the activation of $GABA_B$ receptors on pre and/or postsynaptic membranes. We

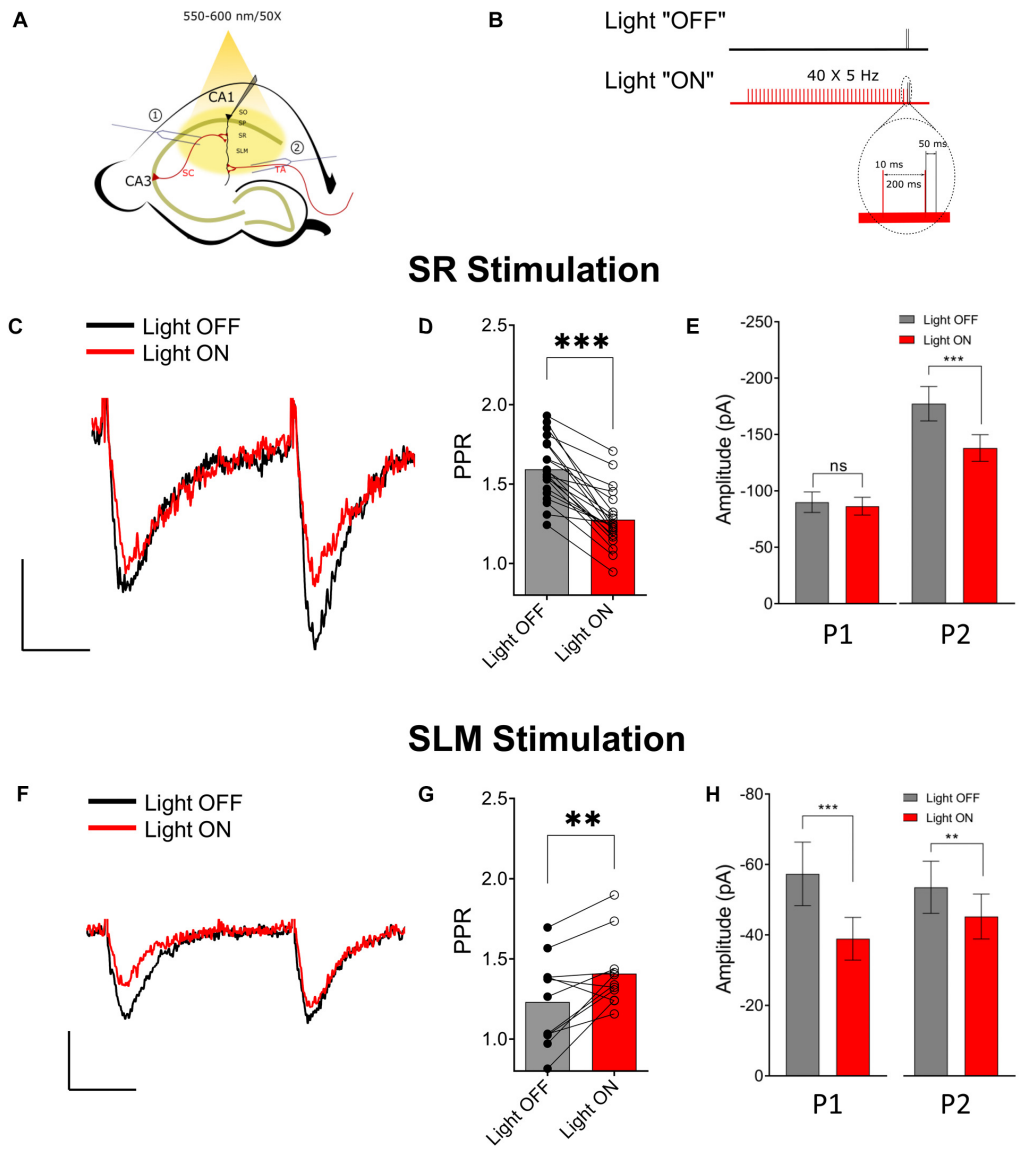

FIGURE 3 | Optogenetically released acetylcholine (ACh) had different effects on Schaffer collateral (SC) and temporoammonic (TA) synaptic inputs. **(A)** Schematic representation of the experimental configuration: the bipolar stimulating electrode was placed either in (1) the stratum radiatum to stimulate the SC or (2) the stratum lacunosum moleculare to stimulate the TA and RE pathways. **(B)** Schematic representation of the experimental paradigm; inset shows magnified view of the region marked by dashed line in the "Light ON" condition to show the temporal relationship between the last two light pulses (in red) and the paired electrical pulses (in black). **(C)** Representative paired-pulse traces from a CA1 pyramidal cell in response to SC stimulation with (red) and without (black) optogenetic stimulation of ACh release. **(D)** Scatter plot of individual data point overlaid on bar plot shows the effect of ACh release on SC PPR (paired *t*-test, $p < 0.001$). **(E)** Bar plots showing that ACh-release caused significant reduction in the amplitude of the second EPSC (P2; paired *t*-test; $p < 0.0001$), but not the first (P1). **(F)** Representative paired-pulse traces from a CA1 pyramidal cell in response to SLM stimulation with (red) and without (black) optogenetic stimulation of ACh release. **(G)** Scatter plot of individual data point overlaid on bar plot to show the effect of ACh release on TA PPR (paired *t*-test, $p = 0.0096$) **(H)** Bar plots showing that ACh-release caused significant reduction in the amplitude of both the first (P1) and the second EPSC (P2) (paired *t*-test; $p < 0.05$ and $p < 0.001$, respectively). Scale bars: $x = 25$ ms; $y = 50$ pA.

first investigated the possibility that ACh release increased the excitability of interneurons that activate postsynaptic $GABA_B$ receptors on CA1 PCs. To do this, we performed experiments with an intracellular recording solution that contained 5 μM GDP-β-S, (instead of GTP) to inhibit postsynaptic G-protein receptor signaling (Bell et al., 2015a). As shown in **Figure 5D** (top panel), the inclusion of GDP-β-S in the patch pipette blocked the ACh mediated reduction of PPR ($p = 0.1589$; $t = 1.576$; df = 7; $n = 8$ cells from five animals). Intracellular GDP-β-S also inhibited baclofen (10 μM) mediated hyperpolarization of CA1 PCs demonstrating its ability to uncouple G-protein signaling (**Figure 5D**, bottom panel; $p < 0.0001$; unpaired *t*-test;

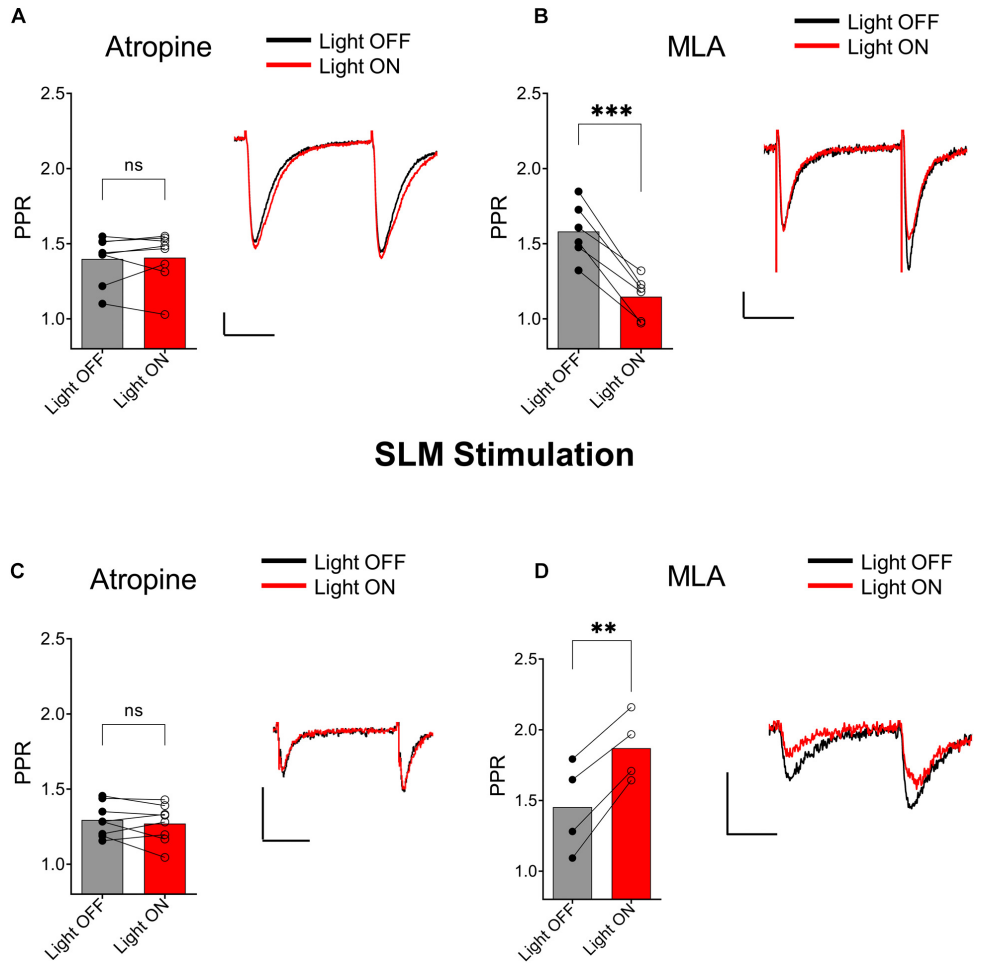

FIGURE 4 | Muscarinic receptor activation mediated synaptic inhibition by ACh release in both the SC and TA pathways. **(A)** Bar plot of SC PPR (left) and representative EPSCs (right) demonstrates that atropine prevented ACh (red) mediated suppression of SC synaptic amplitudes and PPR (paired *t*-test; $p = 0.7629$). **(B)** Bar plot of SC PPR (left) and representative EPSCs show MLA had no effect on ACh (red) mediated inhibition of SC EPSCs and PPR (paired *t*-test; $p = 0.0007$). Scale bars: $x = 20$ ms; $y = 50$ pA. **(C)** Bar plot of SLM PPR (left) and representative EPSCs (right) show atropine blocked both the ACh (red) mediated inhibition of SLM EPSC amplitudes and increase in SLM PPR (paired *t*-test; $p = 0.7159$). **(D)** Bar plot of SLM PPR (left) and representative EPSCs (right) show MLA did not prevent the effect of ACh release on SLM EPSC amplitudes or SLM PPR (paired *t*-test; $p = 0.0036$). Scale bars: $x = 20$ ms; $y = 50$ pA.

$t = 19.67$ df $= 8$; $n = 6$ cells for GDP-β-S, and four cells for control). Therefore, these data suggested that ACh-mediated reduction of PPR in the SR was mediated through the activation of postsynaptic $GABA_B$ receptors.

Finally, we tested whether optogenetically released ACh can increase the excitability of hippocampal CA1 interneurons to SC excitatory afferents. To do this we used the same stimulation paradigm outlined in **Figures 3A,B**. At the beginning of each experiment, we adjusted the strength of the electrical stimulation so that paired SC electrical stimulation resulted in subthreshold depolarizations. As shown in **Figure 5E**, paired pulse stimulation of SC afferents resulted in subthreshold EPSPs in a postsynaptic interneuron (**Figure 5E**, gray trace). However, a train of 40 X 5 Hz yellow light pulses preceding electrical stimulation resulted in a slow subthreshold depolarization of the interneuron membrane potential and the production of APs following electrical stimulation of SC afferents (**Figure 5E**, red trace). Analysis of paired recordings of four neurons from three mice showed that ACh-release rendered a sub-population of CA1 interneurons more likely to discharge in response to stimulation of the SC pathway (**Figure 5E**; two-way ANOVA; significant effect of light: $p < 0.0001$; $F(1, 6) = 147.4$; $n = 4$ cells from three animals). These data suggest that the release of ACh depolarizes a subset of hippocampal interneurons that results in an increase in their excitability to SC synaptic inputs. These interneurons presumably release GABA onto $GABA_B$ receptors located on postsynaptic CA1 PCs.

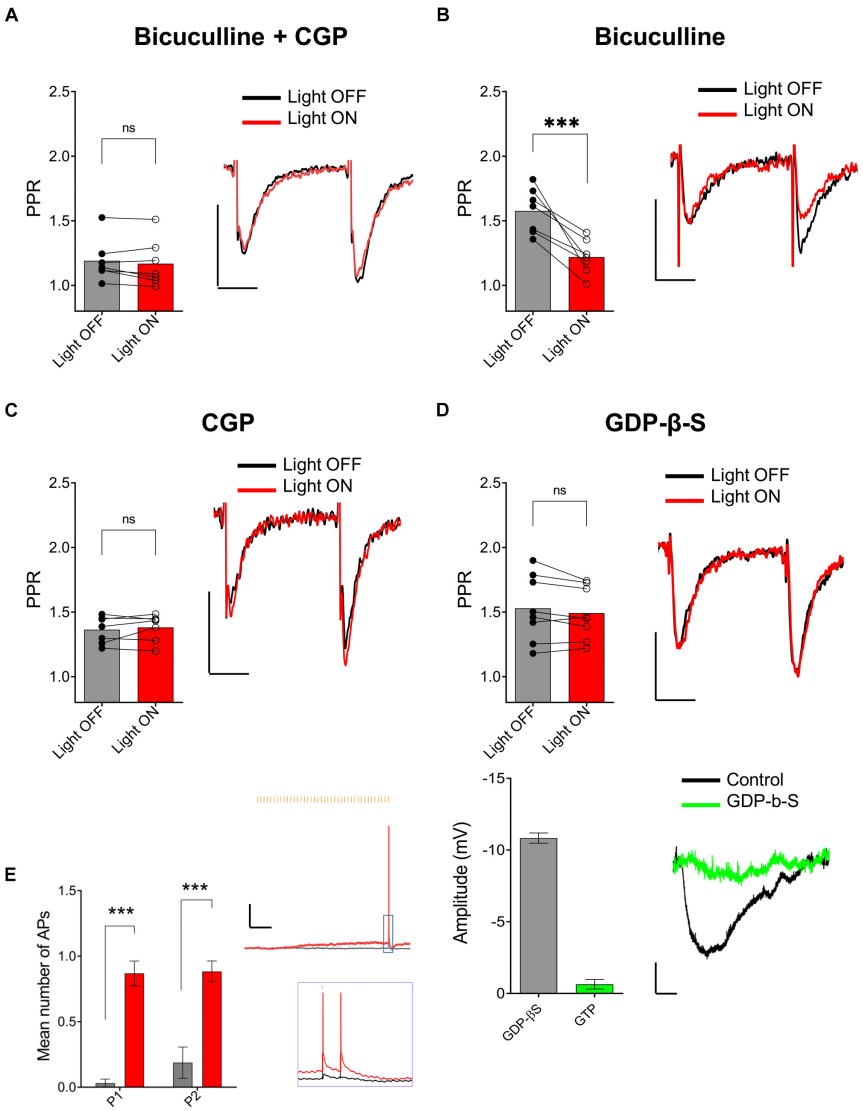

FIGURE 5 | ACh-mediated inhibition of SC inputs required activation of postsynaptic $GABA_B$ receptors. **(A)** Bar plot (left) and representative EPSCs (right) showing ACh-mediated inhibition of SC EPSCs was prevented by $GABA_A$ antagonist bicuculline (BIC) and $GABA_B$ antagonist CGP 52432 (paired *t*-test; $p = 0.2440$); **(B)** Bar plot (left) and representative EPSCs (right) showing BIC alone had no effect on ACh-mediated inhibition of SC EPSCs (paired *t*-test; $p = 0.8332$); **(C)** Bar plot (left) and representative EPSCs (right) showing ACh-mediated inhibition of SC EPSCs was blocked by bath application of CGP 52432 alone (paired *t*-test; $p = 0.0023$); **(D)** Upper, Bar plot (left) and representative EPSCs (right) demonstrate that inclusion of GDP-β-S in the patch pipette prevented ACh-mediated reduction of SC EPSCs (paired *t*-test; $p = 0.1589$). Scale bars: $x = 20$ ms; $y = 50$ pA. Lower, Bar plot (left) showing that hyperpolarization produced in CA1 PCs by the $GABA_B$ receptor agonist baclofen was prevented when including GDP-β-S in the intracellular solution (green bar). Representative membrane potential responses (Right) to baclofen in PCs recorded with intracellular solution containing GTP (black) or GDP-β-S (green); scale bars: $x = 100$ s; $y = 2$ mV. **(E)** Bar plots (on left) and representative traces (on right) showing that ACh-release increased the probability that CA1 interneurons produced APs in response to the paired electrical impulses delivered to the SR. Inset shows magnified image of traces indicated by the blue box. Black trace: light OFF, Red trace: Light ON; scale bars: $x = 1000$ ms; $y = 5$ mV (2-way ANOVA: significant effect of light stimulation; $p < 0.0001$).

$GABA_B$-Mediated Inhibition of Excitatory Synaptic Transmission in SR Is Mediated by the Activation of Inwardly Rectifying Potassium Channels

Because postsynaptic $GABA_B$ receptors can mediate some of their actions through the activation of G-protein coupled inwardly rectifying potassium channels (GIRKs) (Lüscher et al., 1997), we tested whether GIRK activation mediated the ACh reduction of PPR in the SR. As a first test, we held CA1 PCs at hyperpolarized holding potentials to remove the intracellular blockade of GIRK channels by Mg^{2+} or polyamines. When we clamped the neurons at −90 mV, a significantly greater reduction of the PPR was observed (**Figure 6A**; $p = 0.0011$; $t = 4.731$ df = 9; $n = 6$ cells held at −90 mV, and five cells held at −70 mV). Next, we attempted to inhibit the GIRK conductance by replacing K^+

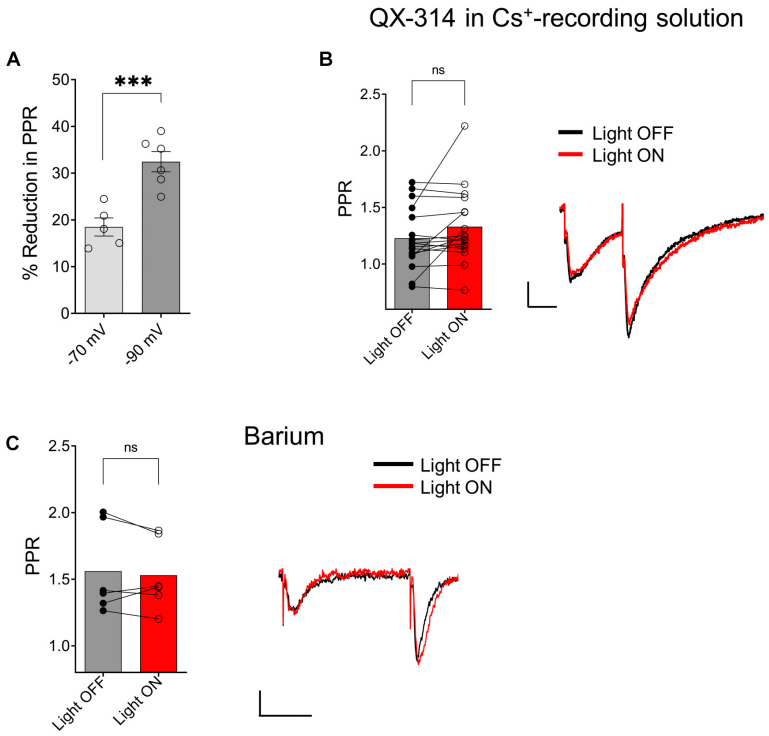

FIGURE 6 | ACh-mediated reduction of SC EPSCs required activation of G-protein coupled inwardly rectifying potassium channels (GIRK). **(A)** Scatter plot of individual data points overlaid on bar plot demonstrating the ACh mediated reduction in SC EPSCs was larger at more negative holding potentials (unpaired *t*-test; $p = 0.0011$). **(B)** Bar plot (left) and representative EPSCs (right) shows inclusion of QX-314 and cesium in the intracellular recording solution prevented inhibition of SC EPSCs by ACh release (paired *t*-test; $p = 0.0758$). **(C)** Bar plot (left) and representative EPSCs (right) shows extracellular barium prevented inhibition of SC EPSCs by ACh release (Paired *t*-test; $p = 0.4984$); Scale bars: $x = 25$ ms; $y = 50$ pA.

with Cs^+ in the intracellular recording solution. The intracellular solution also contained 10 mM QX-314, a blocker of voltage activated Na^+ channels and GIRK channels (Andrade, 1991). Under these conditions the effect of ACh on PPR in the SR was abolished (**Figure 6B**, $p = 0.0758$; $t = 1.899$; df = 16; $n = 17$ cells from six animals). To further test the involvement of the GIRK channels, we attempted to directly inhibit the GIRK conductance via extracellular application of Ba^{2+} (200 μM) (Breton and Stuart, 2017). As shown in **Figure 6C**, extracellular application of Ba^{2+} blocked the ACh-mediated reduction of PPR (**Figure 6C**; $p = 0.4984$; $t = 0.7296$; df = 5; $n = 6$ cells from three animals). Therefore, our data suggest that ACh release increases the excitability of inhibitory interneurons that activate GIRK channels on CA1 PCs through the activation of $GABA_B$ receptors.

ACh Release Inhibits Synaptic Transmission in Excitatory Inputs in the SR and SLM via the Activation of Different Muscarinic Receptor Subtypes

Muscarinic receptors can be categorized into two groups, excitatory muscarinic receptors (M_1, M_3, and M_5) that are coupled to $G_{q/11}$ type G-proteins and inhibitory muscarinic receptors (M_2 and M_4) that have been shown to inhibit transmitter release via the activation of $G_{i/o}$ type G-proteins (Levey and Edmunds, 1995). Because the ACh-mediated inhibition of synaptic transmission in SR appears to involve an increase in inhibitory interneuron excitability, we tested the involvement of the M_1 and M_3 muscarinic receptors. To do this, we included the M_1-selective antagonists VU 0255035 (10 μM) or the M_3 receptor antagonist 4-DAMP (100 nM) in the bath. As shown in **Figure 7A**, the inclusion of VU 0255035 in the perfusate did not have an effect on the ACh-mediated reduction of PPR ($p = 0.0061$; $t = 4.136$; df = 6; $n = 7$ from three animals). In contrast, 4-DAMP blocked the effect of ACh on synaptic transmission in SR (**Figure 7B**; $p = 0.2209$; $t = 1.449$; df = 4; $n = 5$ from three animals). Therefore, these data suggest that ACh release inhibited synaptic transmission in the SR through an increase in interneuron excitability via the activation of M_3-muscarinic receptors.

We next investigated whether inhibition of excitatory inputs in the SLM was mediated by M_2 or M_4 muscarinic receptors. Application of the M_2 receptor antagonist AF-DX 116 (500 nM) significantly blocked the ACh-mediated inhibition of synaptic transmission (**Figure 7C**; $p = 0.1984$; $t = 1.540$; df = 4; $n = 5$ from three animals). In contrast, antagonism of the M_4 receptor by PD102807 (1 μM) had no effect on the PPR (**Figure 7D**,

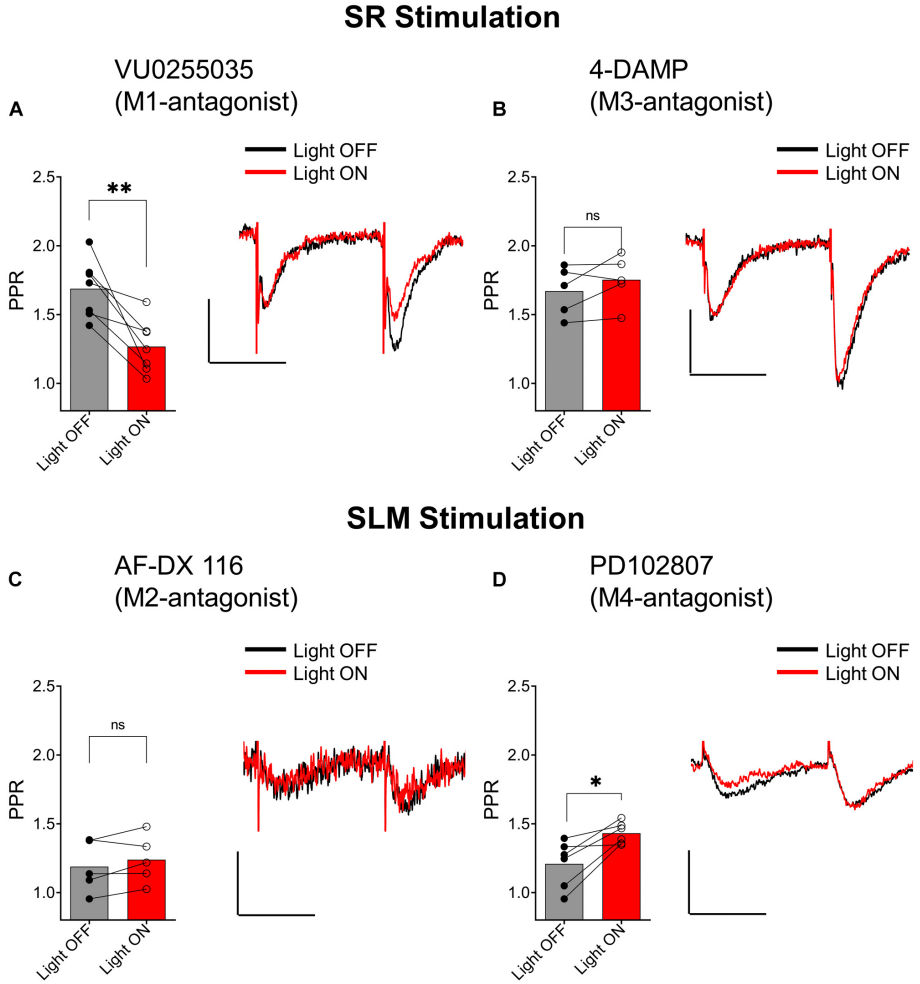

FIGURE 7 | Distinct subtypes of muscarinic receptors mediated the inhibition of EPSCs in the SR and SLM. **(A)** Bar plot (left) and representative EPSCs (right) demonstrate that VU0255035 (M1 antagonist) had no effect on inhibition of SC EPSCs by ACh release (paired *t*-test; $p = 0.0061$). **(B)** Bar plot (left) and representative EPSCs (right) demonstrate inhibition of SC EPSCs by ACH release is prevented by 4-DAMP (M3 antagonist) (paired *t*-test; $p = 0.2209$). **(C)** Bar plot (left) and representative EPSCs (right) demonstrate that AF-DX 116 (M2 antagonist) prevented ACh-mediated inhibition of SLM EPSCs (paired *t*-test; $p = 0.1984$). **(D)** Bar plot (left) and representative EPSCs (right) demonstrate PD 102807 (M4-antagonist) had no effect on TA EPSC suppression by ACh release (paired *t*-test; $p = 0.0138$); Scale bars: $x = 20$ ms; $y = 50$ pA.

$p = 0.0138$; $t = 3.711$; df = 5; $n = 6$ from three animals). Therefore, these data suggest ACh release inhibited synaptic inputs in the SLM through the activation of M_2 receptors.

DISCUSSION

In the present study, we demonstrate that low-frequency optogenetic stimulation of cholinergic terminals suppressed glutamatergic neurotransmission in the SR and SLM via different cellular and network mechanisms. ACh release indirectly inhibited SR inputs by increasing the excitability of CA1 interneurons that postsynaptically activated $GABA_B$ receptors and GIRK channels on CA1 PCs. Furthermore, the ACh increase in CA1 interneuron excitability was mediated by the activation of M_3 muscarinic receptors. In contrast, ACh release inhibited inputs in the SLM through the activation of M_2 muscarinic receptors, likely located on the presynaptic terminals. Thus, our data have uncovered a previously unrecognized network mechanism by which ACh release controls SC inputs in hippocampal CA1 PCs through the modulation of interneuron excitability.

Previous studies from our lab (Bell et al., 2011, 2013, 2015a) and others (Zhenglin and Yakel, 2011; Alger et al., 2014) have studied the effects of ACh release on hippocampal function by utilizing virally mediated expression of blue light activated channelrhodopsin variants in MS/DBB cholinergic neurons. However, this approach may have limitations as blue light might not penetrate sufficiently far into tissue so that some cholinergic terminals are not be activated by light flashes. Furthermore, intracranial viral transfection may not sufficiently transfect all cholinergic neurons that project to the hippocampus due to

imperfect targeting of the MS/DBB. In the present paper, we have taken a different approach in which the excitatory optogenetic protein ReaChR (Lin et al., 2013) was selectively expressed in cholinergic neurons through crossing a Cre-dependent ReaChR reporter mouse line (Hooks et al., 2015) to a cholinergic Cre-driver mouse line (Rossi et al., 2011). This has two potential advantages. First, ReaChR's activation spectrum is red-shifted so that longer wavelength light can be used to penetrate further into tissue and excite more cholinergic terminals in a brain slice. Second, all cholinergic neurons that project to the hippocampus appear to express ReaChR. Using this approach, we demonstrated that ReaChR-expressing neurons in MS/DBB could be activated by yellow light pulses. More importantly, optogenetic stimulation of cholinergic terminals in hippocampal brain slices produced responses in hippocampal CA1 interneurons previously reported by others using electrical (Widmer et al., 2006) and blue light optogenetic stimulation (Bell et al., 2013). Therefore, by using genetically modified mouse driver and reporter lines, we can reliably release ACh from MS/DBB cholinergic terminals in hippocampal CA1 brain slices. Although, it is possible that higher frequencies of stimulation may lead to increased ACh release that could potentially uncover a presynaptic muscarinic component in the SR (Hasselmo and Schnell, 1994) we did not test higher frequency of stimulation due to two reasons: Firstly, the slower channel closing kinetics of ReaChR does not permit higher stimulation frequencies (Lin et al., 2013), and secondly, a number of studies have indicated that septal cholinergic neurons typically fire at a low frequency (Simon, 2006; Zhang et al., 2011). Furthermore, the inhibition of acetylcholinesterases by donepezil in our studies, which should increase extracellular ACh beyond physiological levels, failed in uncovering a presynaptic muscarinic component in the SR.

A small number of studies have investigated cholinergic receptor modulation of excitatory inputs in the SLM of hippocampal CA1 (Hasselmo and Schnell, 1994; Thorn et al., 2017). Our studies extended these studies by being the first to investigate modulation of synaptically released ACh on excitatory afferents in SLM. Consistent with studies utilizing bath application of cholinergic agonists, we observed that ACh release suppressed excitatory inputs in SLM (Hasselmo and Schnell, 1994; Thorn et al., 2017). Furthermore, ACh release appeared to act presynaptically as the inhibition of afferents in SLM was accompanied by an increase in the PPR, which is frequently used to determine presynaptic function. We further extended previous studies by demonstrating that suppression of SLM inputs by ACh release was mediated by muscarinic M_2 receptor activation. These latter findings were consistent with observations from a recent study that suggest that presynaptic inhibition at synapses in the SLM was not mediated by M_4 muscarinic receptors (Thorn et al., 2017). Therefore, our data confirms and extends observation made by previous studies and suggest that ACh release from MS/DBB cholinergic terminals results in presynaptic inhibition of inputs in the SLM via the activation of M_2 receptors.

Several studies have investigated cholinergic modulation of SR inputs in hippocampal CA1 (Valentino and Dingledine, 1981; Hasselmo and Schnell, 1994; Kremin et al., 2006). Most studies utilized exogenous activation of muscarinic receptors that resulted in presynaptic inhibition of glutamate release from excitatory terminals in SR (Valentino and Dingledine, 1981; Sheridan and Sutor, 1990; Hasselmo and Schnell, 1994; Kremin et al., 2006; Dasari and Gulledge, 2011). Other studies that have utilized electrical stimulation to release ACh have confirmed that endogenous ACh caused a presynaptic inhibition of CA1 SR inputs through the activation of muscarinic receptors (Fernández de Sevilla and Buño, 2003). In our study, we also assessed the effect of ACh release on SR inputs in hippocampal CA1 using optogenetic stimulation. However, we observed no effect of ACh release on the first electrically evoked SC EPSC in a pair of stimuli. In contrast, the second EPSC of the paired stimulation was suppressed by ACh release. The suppression of the second EPSC was prevented by blockade of postsynaptic G-protein function, $GABA_B$ receptor antagonists, GIRK channel inhibition, or by M_3 receptor inhibition. Thus, our data suggested that the primary effect of ACh release on SC inputs was to increase the excitability of a subset of interneurons via an M_3 receptor-mediated mechanism. These interneurons through a combination of M_3 receptor-mediated increase in excitability and feedforward excitation by SR inputs drove the interneurons to spike and release GABA onto $GABA_B$ receptors of CA1 PCs. The $GABA_B$ receptor activation then activated GIRK channels on CA1 PCs and inhibited SC inputs onto these same cells. Indeed, GABA released by the interneurons could potentially activate both $GABA_A$ as well as $GABA_B$ receptors expressed on CA1 principal cells. However, in the present study the CA1 principal cells were held at −70 mV, which is close to the equilibrium potential for $GABA_A$ receptors (Kuffler and Edwards, 1958). Therefore, the shunting effects of $GABA_A$ receptor activation should be reduced or eliminated in voltage clamp mode. This would permit the examination of postsynaptic $GABA_B$ modulation in isolation. Although we do not discount contributions of $GABA_A$ receptor activation following ACh release (Pitler and Alger, 1992; Alger et al., 2014; Bell et al., 2015a), these data have identified a novel mechanism by which ACh release affects SC synaptic inputs in the SR of hippocampal CA1.

Despite the role of $GABA_B$ receptor activation of GIRK channels in suppressing SR inputs onto CA1 PCs, no outward current or conductance change accompanied the postsynaptic inhibition. This observation is difficult to reconcile with well described $GABA_B$ inhibitory synaptic potentials (IPSPs) measured in CA1 PCs (Dutar and Nicoll, 1988). However, this observation is consistent with the demonstration that $GABA_B$ receptors form a tight complex with Rgs7, Gβ5 and GIRK2 channels in CA1 PC dendritic spines (Fajardo-Serrano et al., 2013). In contrast, $GABA_B$ receptors are segregated from this complex in dendritic shafts, which suggests that in CA1 PC dendrites $GABA_B$ activation of GIRK channels maybe primarily confined to the dendritic spines. Considering that GIRK2 channels appear to be necessary for $GABA_B$ IPSP activation in CA1 PCs, it is possible that the $GABA_B$-mediated postsynaptic inhibition of SR inputs measured in our studies was confined to the synaptic spine and conductance changes could not be measured at the soma (Marron Fernandez de Velasco et al., 2017). Thus, suppression of SR inputs in individual spines of CA1 PCs

may provide a mechanism for selective inhibition of individual synapses on CA1 PCs.

Our results differ from previous studies that have investigated muscarinic modulation of SC inputs in hippocampal CA1. These differences could arise for a number of possible reasons. First, because there is a non-uniform density of cholinergic afferents and acetylcholinesterase in hippocampal CA1 (Aznavour et al., 2002; Franklin and Paxinos, n.d.), uniform exogenous application of cholinergic agonists may activate presynaptic muscarinic receptors that are not normally activated by endogenous ACh. This is supported by the observation that the concentration of acetylcholine varies in different layers of the hippocampus during increased acetylcholine release (Zhang et al., 2010). Second, studies that observed presynaptic muscarinic receptor-mediated inhibition of the pathways in the SR following electrically released ACh were performed at 20–22°C, in the presence of the acetylcholinesterase inhibitor physostigmine, and a $GABA_A$ receptor antagonist (Fernández de Sevilla and Buño, 2003). In contrast, we performed our studies at 32–34°C either in the absence of any inhibitors or in the presence of the acetylcholinesterase inhibitor donepezil. Importantly, acetylcholinesterase isoforms are temperature sensitive and the acetylcholinesterase inhibitors physostigmine and donepezil have different affinities for the varying isoforms of acetylcholinesterase expressed in the hippocampus (Zhao and Tang, 2002). Thus, the studies performed at colder temperatures in the presence of physostigmine may have permitted ACh release to diffuse farther from cholinergic synapses and activate presynaptic muscarinic receptors on terminals in the SR that under our conditions could not be activated. Thus, it is unclear whether the observations made in the presence of physostigmine and colder temperatures uncovered an effect of ACh release that normally occurs physiologically or only happens under conditions of acetylcholinesterase inhibition such as in the treatment of AD patients. Nevertheless, our results in the absence of acetylcholinesterase inhibitors and at more physiological temperatures suggest that ACh release affects excitatory inputs in the SR by increasing the excitability of inhibitory interneurons and facilitating feedforward inhibition, which activate $GABA_B$ receptors and GIRK channels on CA1 PCs.

In addition to presynaptic inhibition by muscarinic receptors, previous studies have demonstrated the presence of α7 nicotinic receptors on terminals in the SR, which when activated by exogenous nicotinic agonists facilitate the release of glutamate (Ji et al., 2001; Maggi et al., 2003; Sola et al., 2006). Moreover, endogenous activation of presynaptic α7 nicotinic receptors has been implicated in the induction of synaptic plasticity at this synapse (Zhenglin and Yakel, 2011; Gu et al., 2012). However, to our knowledge there have been no studies that demonstrate that ACh release can potentiate glutamate release from CA1 SC terminals on a timescale of an individual synaptic event. Our data suggest that ACh cannot potentiate the release of glutamate from SC or TA terminals in hippocampal CA1 when coupled with an individual presynaptic AP. However, our data did not examine the possibility that presynaptic nicotinic receptors modify synaptic strength on a long term timescale such as that which occurs with long-term potentiation (Zhenglin and Yakel, 2011).

CONCLUSION

In conclusion, our data have shown that optogenetically released ACh in mouse hippocampal slices differentially inhibited glutamatergic synaptic transmission onto CA1 PCs depending on the input. Inputs in the SLM of CA1 were presynaptically inhibited by ACh release onto M_2 muscarinic receptors as previously demonstrated by others. In contrast, inputs in the SR of CA1 were not directly modulated by ACh release. Instead, ACh release increased the excitability of a subset of interneurons that synapse on CA1 PCs, through an M_3 muscarinic receptor-mediated mechanism. This increased interneuron excitability facilitated feedforward inhibition that resulted in postsynaptic inhibition via $GABA_B$ receptor activation of GIRK channels. Thus, ACh modulation of CA1 SC inputs would depend on the amount of ongoing activity of SC inputs and may occur at the level of an individual spine.

CONTRIBUTION TO THE FIELD STATEMENT

Previous studies have demonstrated that steady-state uniform activation of cholinergic receptors in hippocampal CA1 resulted in greater muscarinic receptor-mediated presynaptic suppression of excitatory inputs in SR compared to those in SLM. However, cholinergic afferent and acetylcholinesterase densities are not uniformly distributed in hippocampal CA1 and thus steady-state pharmacological cholinergic receptor activation unlikely mimics ACh release. Following optogenetic ACh release, we confirmed muscarinic receptor-mediated presynaptic inhibition of excitatory inputs in SLM. In contrast, SR excitatory inputs were postsynaptically inhibited by ACh release through an increase in inhibitory interneuron excitability, which resulted in $GABA_B$ receptor activation of inwardly rectifying potassium channels on CA1 pyramidal neurons. Together, our data demonstrate novel muscarinic receptor and circuit mechanisms that differentially modulate distinct excitatory inputs following ACh release.

DATA AVAILABILITY

All datasets generated for this study are included in the manuscript and/or the supplementary files.

ETHICS STATEMENT

Mice used in these studies were housed in an animal care facility approved by the American Association for the Accreditation of Laboratory Animal Care (AAALAC). Animal experimental procedures followed a protocol approved by the Institutional Animal Care and Use Committee of Virginia Commonwealth

University (AD 20205). This protocol adhered to the ethical guidelines described in The Care and Use of Laboratory Animals, 8th Edition. Efforts were made to minimize animal suffering and to reduce the number of animals used.

AUTHOR CONTRIBUTIONS

PG designed the experiments, acquired and analyzed the data, and wrote the manuscript. ARM performed the experiments, conceived and directed the research, reviewed the data, and wrote and edited the manuscript. Both the authors read, reviewed, and approved the final version of the manuscript.

FUNDING

In this work, ARM was financially supported by the NIH grants R21AG055073 and R01MH107507.

REFERENCES

Alger, B. E., Nagode, D. A., and Tang, A.-H. (2014). Muscarinic cholinergic receptors modulate inhibitory synaptic rhythms in hippocampus and neocortex. *Front. Synapt. Neurosci.* 6:18. doi: 10.3389/fnsyn.2014.00018

Andrade, R. (1991). Blockade of neurotransmitter-activated K+ conductance by QX-314 in the Rat hippocampus. *Eur. J. Pharmacol.* 199, 259–262. doi: 10.1016/0014-2999(91)90467-5

Araque, A., Martìn, E. D., Perea, G., Arellano, J. I, and Buño, W. (2002). Synaptically released acetylcholine evokes Ca 2+ elevations in astrocytes in hippocampal slices. *J. Neurosci.* 22, 2443–2450. doi: 10.1523/JNEUROSCI.22-07-02443.2002

Aznavour, N., Mechawar, N., and Descarries, L. (2002). Comparative analysis of cholinergic innervation in the dorsal hippocampus of adult mouse and rat: a quantitative immunocytochemical study. *Hippocampus* 12, 206–217. doi: 10.1002/hipo.1108

Bell, K. A., Shim, H., Chen, C.-K., and McQuiston, A. R. (2011). Nicotinic excitatory postsynaptic potentials in hippocampal ca1 interneurons are predominantly mediated by nicotinic receptors that contain Alpha4 and Beta2 Subunits. *Neuropharmacology* 61, 1379–1388. doi: 10.1016/j.neuropharm.2011.08.024

Bell, L. A., Bell, K. A., and McQuiston, A. R. (2013). Synaptic muscarinic response types in hippocampal ca1 interneurons depend on different levels of presynaptic activity and different muscarinic receptor subtypes. *Neuropharmacology* 73, 160–173. doi: 10.1016/j.neuropharm.2013.05.026

Bell, L. A., Bell, K. A., and McQuiston, A. R. (2015b). Activation of muscarinic receptors by ach release in hippocampal CA1 depolarizes vip but has varying effects on parvalbumin-expressing basket cells: endogenous muscarinic receptor activation and perisomatic interneurons. *J. Physiol.* 593, 197–215. doi: 10.1113/jphysiol.2014.277814

Bell, L. A., Bell, K. A., and McQuiston, A. R. (2015a). Acetylcholine release in mouse hippocampal CA1 preferentially activates inhibitory-selective interneurons via A4β2* nicotinic receptor activation. *Front. Cell. Neurosci.* 9:115. doi: 10.3389/fncel.2015.00115

Brazhnik, E. S., and Fox, S. E. (1997). Intracellular recordings from medial septal neurons during hippocampal theta rhythm. *Exp. Brain Res.* 114, 442–453. doi: 10.1007/PL00005653

Breton, J.-D., and Stuart, G. J. (2017). GABA B receptors in neocortical and hippocampal pyramidal neurons are coupled to different potassium channels. *Eur. J. Neurosci.* 46, 2859–2866. doi: 10.1111/ejn.13777

Buño, W., Cabezas, C., and de Sevilla, D. F. (2006). Presynaptic muscarinic control of glutamatergic synaptic transmission. *J. Mol. Neurosci.* 30, 161–164. doi: 10.1385/jmn:30:1:161

Cole, A., and Nicoll, R. (1983). Acetylcholine mediates a slow synaptic potential in hippocampal pyramidal cells. *Science* 221, 1299–1301. doi: 10.1126/science.6612345

Dasari, S., and Gulledge, A. T. (2011). M1 and M4 receptors modulate hippocampal pyramidal neurons. *J. Neurophysiol.* 105, 779–792. doi: 10.1152/jn.00686.2010

Dutar, P., and Nicoll, R. A. (1988). A physiological role for gaba8 receptors in the central nervous system. *Nature* 332, 156–158. doi: 10.1038/332156a0

Fajardo-Serrano, A., Wydeven, N., Young, D., Watanabe, M., Shigemoto, R., Martemyanov, K. A., et al. (2013). Association of Rgs7/Gβ5 complexes with girk channels and GABA B receptors in hippocampal CA1 pyramidal neurons: subcellular localization OF Rgs7 and Gβ5 in the hippocampus. *Hippocampus* 23, 1231–1245. doi: 10.1002/hipo.22161

Fernández de Sevilla, D., and Buño, W. (2003). Presynaptic inhibition of schaffer collateral synapses by stimulation of hippocampal cholinergic afferent fibres: presynaptic cholinergic inhibition. *Eur. J. Neurosci.* 17, 555–558. doi: 10.1046/j.1460-9568.2003.02490.x

Franklin, K., and Paxinos, G. (n.d.). *The Mouse Brain in Stereotaxic Coordinates*.

Frazier, C. J., Rollins, Y. D., Breese, C. R., Leonard, S., Freedman, R., and Dunwiddie, T. V. (n.d.). Acetylcholine activates an ?-bungarotoxin-sensitive nicotinic current in rat hippocampal interneurons, but not pyramidal cells.

Gu, Z., Lamb, P. W., and Yakel, J. L. (2012). Cholinergic coordination of presynaptic and postsynaptic activity induces timing-dependent hippocampal synaptic plasticity. *J. Neurosci.* 32, 12337–12348. doi: 10.1523/JNEUROSCI.2129-12.2012

Hampel, H., Mesulam, M. M., Cuello, A. C., Farlow, M. R., Giacobini, E., Grossberg, G. T., et al. (2018). The cholinergic system in the pathophysiology and treatment of alzheimer's disease. *Brain* 141, 1917–1933. doi: 10.1093/brain/awy132

Hasselmo, M., and Schnell, E. (1994). Laminar selectivity of the cholinergic suppression of synaptic transmission in rat hippocampal region CA1: computational modeling and brain slice physiology. *J. Neurosci.* 14, 3898–3914. doi: 10.1523/JNEUROSCI.14-06-03898.1994

Hasselmo, M. E. (2006). The role of acetylcholine in learning and memory. *Curr. Opin. Neurobiol.* 16, 710–715. doi: 10.1016/j.conb.2006.09.002

Hooks, B. M., Lin, J. Y., Guo, C., and Svoboda, K. (2015). Dual-channel circuit mapping reveals sensorimotor convergence in the primary motor cortex. *J. Neurosci.* 35, 4418–4426. doi: 10.1523/JNEUROSCI.3741-14.2015

Ji, D., Lape, R., and Dani, J. A. (2001). Timing and location of nicotinic activity enhances or depresses hippocampal synaptic plasticity. *Neuron* 31, 131–141. doi: 10.1016/S0896-6273(01)00332-334

Jones, S., and Yakel, J. L. (1997). Functional nicotinic ach receptors on interneurones in the rat hippocampus. *J. Physiol.* 504, 603–610. doi: 10.1111/j.1469-7793.1997.603bd.x

Kremin, T., Gerber, D., Giocomo, L., Huang, S., Tonegawa, S., and Hasselmo, M. (2006). Muscarinic suppression in stratum radiatum of CA1 shows dependence on presynaptic M1 receptors and is not dependent on effects at GABAB receptors. *Neurobiol. Learn. Mem.* 85, 153–163. doi: 10.1016/j.nlm.2005.09.005

Kuffler, S. W., and Edwards, C. (1958). Mechanism of gamma aminobutyric acid (Gaba) action and its relation to synaptic inhibition. *J. Neurophysiol.* 21, 589–610. doi: 10.1152/jn.1958.21.6.589

Levey, I., and Edmunds, M. (1995). Expression of Ml-M4 muscarinic acetylcholine receptor proteins in rat hippocampus and regulation by cholinergic innervation. *J. Neurosci.* 15, 4077–4092. doi: 10.1523/jneurosci.15-05-04077.1995

Lin, J. Y., Knutsen, P. M., Muller, A., Kleinfeld, D., and Tsien, R. Y. (2013). ReaChR: a red-shifted variant of channelrhodopsin enables deep transcranial optogenetic excitation. *Nat. Neurosci.* 16, 1499–1508. doi: 10.1038/nn.3502

Lüscher, C., Jan, L. Y., Stoffel, M., Malenka, R. C., and Nicoll, R. A. (1997). G protein-coupled inwardly rectifying K+ channels (Girks) mediate postsynaptic but not presynaptic transmitter actions in hippocampal neurons. *Neuron* 19, 687–695. doi: 10.1016/S0896-6273(00)80381-80385

Maggi, L., Le Magueresse, C., Changeux, J.-P., and Cherubini, E. (2003). Nicotine activates immature 'silent'. connections in the developing hippocampus. *Proc. Natl. Acad. Sci.* 100, 2059–2064. doi: 10.1073/pnas.0437947100

Marron Fernandez de Velasco, E., Zhang, L. N., Vo, B., Tipps, M., Farris, S., Xia, Z., et al. (2017). GIRK2 splice variants and neuronal G protein-gated K+ channels: implications for channel function and behavior. *Sci. Rep.* 7:1639. doi: 10.1038/s41598-017-01820-1822

McQuiston, A. R., and Madison, D. V. (1999c). Nicotinic receptor activation excites distinct subtypes of interneurons in the rat hippocampus. *J. Neurosci.* 19, 2887–2896. doi: 10.1523/JNEUROSCI.19-08-02887.1999

McQuiston, A. R., and Madison, D. V. (1999a). Muscarinic receptor activity has multiple effects on the resting membrane potentials of CA1 hippocampal interneurons. *J. Neurosci.* 19, 5693–5702. doi: 10.1523/JNEUROSCI.19-14-05693.1999

McQuiston, A. R., and Madison, D. V. (1999b). Muscarinic receptor activity induces an afterdepolarization in a subpopulation of hippocampal CA1 interneurons. *J. Neurosci.* 19, 5703–5710. doi: 10.1523/JNEUROSCI.19-14-05703.1999

Parra, P., Gulyás, A. I., and Miles, R. (1998). How many subtypes of inhibitory cells in the hippocampus? *Neuron* 20, 983–993. doi: 10.1016/S0896-6273(00)80479-80471

Pitler, T. A., and Alger, B. E. (1992). Cholinergic excitation of GABAergic interneurons in the rat hippocampal slice. *J. Physiol.* 450, 127–142. doi: 10.1113/jphysiol.1992.sp019119

Qian, J., and Saggau, P. (1997). Presynaptic inhibition of synaptic transmission in the rat hippocampus by activation of muscarinic receptors: involvement of presynaptic calcium influx. *Br. J. Pharmacol.* 122, 511–519. doi: 10.1038/sj.bjp.0701400

Rossi, J., Balthasar, N., Olson, D., Scott, M., Berglund, E., Lee, C. E., et al. (2011). Melanocortin-4 receptors expressed by cholinergic neurons regulate energy balance and glucose homeostasis. *Cell Metab.* 13, 195–204. doi: 10.1016/j.cmet.2011.01.010

Sheridan, R. D., and Sutor, B. (1990). Presynaptic M1 muscarinic cholinoceptors mediate inhibition of excitatory synaptic transmission in the hippocampus in vitro. *Neurosci. Lett.* 108, 273–278. doi: 10.1016/0304-3940(90)90653-q

Simon, A. P. (2006). Firing properties of anatomically identified neurons in the medial septum of anesthetized and unanesthetized restrained rats. *J. Neurosci.* 26, 9038–9046. doi: 10.1523/JNEUROSCI.1401-06.2006

Sola, E., Capsoni, S., Rosato-Siri, M., Cattaneo, A., and Cherubini, E. (2006). Failure of nicotine-dependent enhancement of synaptic efficacy at schaffer-collateral CA1 Synapses of AD11 anti-nerve growth factor transgenic mice. *Eur. J. Neurosci.* 24, 1252–1264. doi: 10.1111/j.1460-9568.2006.04996.x

Thorn, C. A., Popiolek, M., Stark, E., and Edgerton, J. R. (2017). Effects of M1 and M4 activation on excitatory synaptic transmission in CA1: THORN. *Hippocampus* 27, 794–810. doi: 10.1002/hipo.22732

Valentino, R. J., and Dingledine, R. (1981). Presynaptic inhibitory effect of acetylcholine in the hippocampus. *J. Neurosci.* 1:784. doi: 10.1523/JNEUROSCI.01-07-00784.1981

Widmer, H., Ferrigan, L., Davies, C. H., and Cobb, S. R. (2006). Evoked slow muscarinic acetylcholinergic synaptic potentials in rat hippocampal interneurons. *Hippocampus* 16, 617–628. doi: 10.1002/hipo.20191

Wu, M. (2004). Hypocretin/orexin innervation and excitation of identified septohippocampal cholinergic neurons. *J. Neurosci.* 24, 3527–3536. doi: 10.1523/JNEUROSCI.5364-03.2004

Wu, M., Hajszan, T., Xu, C., Leranth, C., and Alreja, M. (2004). Group I metabotropic glutamate receptor activation produces a direct excitation of identified septohippocampal cholinergic neurons. *J. Neurophysiol.* 92, 1216–1225. doi: 10.1152/jn.00180.2004

Zhang, H., Lin, S.-C., and Nicolelis, M. A. L. (2010). Spatiotemporal coupling between hippocampal acetylcholine release and theta oscillations in vivo. *J. Neurosci.* 30, 13431–13440. doi: 10.1523/JNEUROSCI.1144-10.2010

Zhang, H., Lin, S.-C., and Nicolelis, M. A. L. (2011). A distinctive subpopulation of medial septal slow-firing neurons promote hippocampal activation and theta oscillations. *J. Neurophysiol.* 106, 2749–2763. doi: 10.1152/jn.00267.2011

Zhao, Q., and Tang, X. C. (2002). Effects of huperzine a on acetylcholinesterase isoforms in vitro: comparison with tacrine, donepezil, rivastigmine and physostigmine. *Eur. J. Pharmacol.* 455, 101–107. doi: 10.1016/s0014-2999(02)02589-x

Zhenglin, G., and Yakel, J. L. (2011). Timing-dependent septal cholinergic induction of dynamic hippocampal synaptic plasticity. *Neuron* 71, 155–165. doi: 10.1016/j.neuron.2011.04.026

Conflict of Interest Statement: The authors declare that the research was conducted in the absence of any commercial or financial relationships that could be construed as a potential conflict of interest.